VOLCANO-ICE INTERACTIONS IN THE PAVONIS MONS GLACIAL DEPOSIT. K. E. Scanlon[1], W. B. Garry[1], and J. W. Head[2], [1]NASA Goddard Space Flight Center, Greenbelt, MD, USA 20771 [2]Brown University, Providence, RI, USA 02912. kathleen.e.scanlon@nasa.gov

Introduction: Glaciovolcanic landforms—i.e., those formed by the interaction of volcanism and ice—inform geologists about the extent, thickness, and thermal regime of past glaciers and ice sheets [e.g.,1]. Given the cold and dry Amazonian climate [e.g., 2], sites where volcanism melted ice are among the few aqueous environments likely to have existed recently at the surface of Mars. The presence of large glacial fan-shaped deposits [FSDs; 3-6] left by ice sheets as recently as ~125-220 Ma [7] on the then-active Tharsis Montes volcanoes [8] suggests abundant opportunities for lava to have interacted with ice.

All three Tharsis Montes FSDs include edifices hundreds of meters high with steeply sloped flanks and relatively flat tops. In addition to this morphometric indicator [e.g., 9], glaciovolcanism in the Tharsis FSDs is evidenced by the presence and distribution of fluvial or wet-based glacial landforms within what were otherwise cold-based glaciers [4, 10-12].

Glaciovolcanic Landforms: While most of the FSDs are heavily mantled by an unconsolidated material, two possible glaciovolcanic landforms in the Pavonis Mons FSD (**Fig. 1**) outcrop from beneath it (e.g., **Fig. 2**). HiRISE [13] images of these outcrops, with resolution as high as ~27 cm px^{-1}, allow us to interpret the type, geometry and glacial setting of volcano-ice interactions at Pavonis Mons at a level of detail that has not yet been possible for Mars.

The W: One such landform, herein called "the W" (**Fig. 2**), is a series of ridges near the center of the deposit previously mapped as knobby facies [4]. A DEM **(Fig. 3)** created using the Ames Stereo Pipeline [15] and two HiRISE images (PSP_002104_1845 and ESP_037047_1845) show many of the ridges to stand hundreds of meters above surrounding terrain. Most outcrops on ridges imaged by HiRISE are layered, but in some cases appear massive, with polygonal fractures [cf. 14]. A few ridge tops feature pit craters.

One ridge in the W (**Fig. 3**) is ~250 m high and triangular in cross-section. A succession of layered material overlies an apparently massive unit. Layered materials originate at the crest of the ridge and dip away from it, draping the massive unit (**Fig. 4**). A channel at the northern end is 5-10 meters deep (**Fig. 5**). A slope map derived from this DEM (**Fig. 6**) shows slopes ~30-40° across most of the ridge, with the steepest slopes at the southeast, up to ~80° at the exposed section of the massive unit. This is consistent with the inferred direction of ice flow in this part of the FSD [cf. 21].

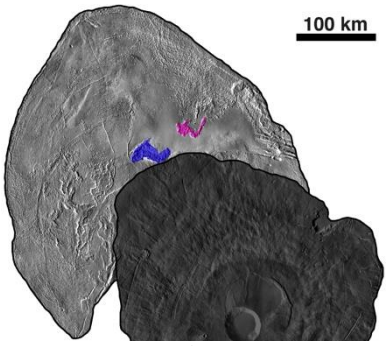

Fig. 1: Pavonis Mons volcano and fan-shaped deposit [17]; the W landform (pink), V landform (blue). THEMIS day IR basemap [18].

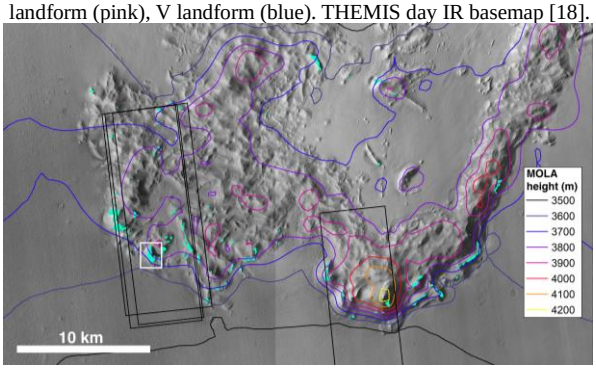

Fig. 2: The W. Outcrops (cyan), HiRISE images (black boxes), Figs. 3-6 (white box). CTX mosaic [19, 20], MOLA contours [16].

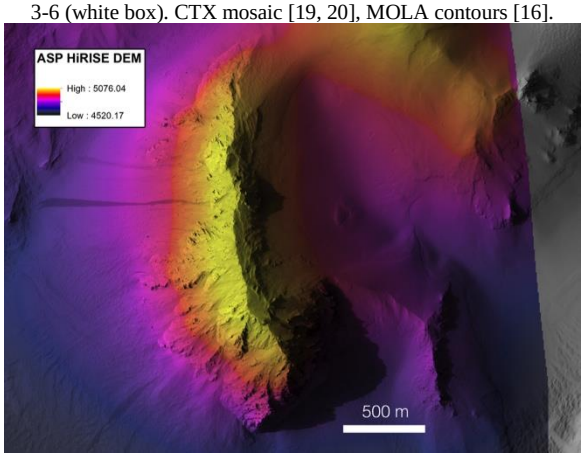

Fig. 3: Glaciovolcanic ridge in the W. HiRISE DEM (Fig. 2).

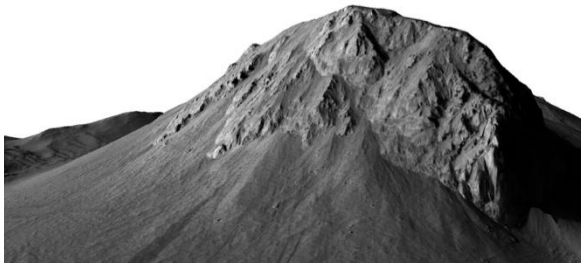

Fig. 4: Perspective view of draped layered materials (Fig. 3). Massive unit in shadow. HiRISE image and DEM.

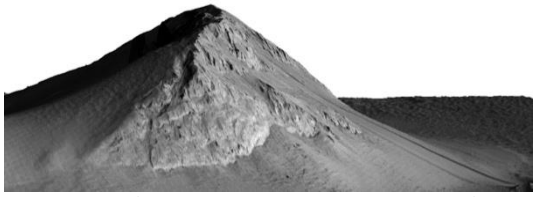

Fig. 5: View of channel incised along northern crest of ridge.

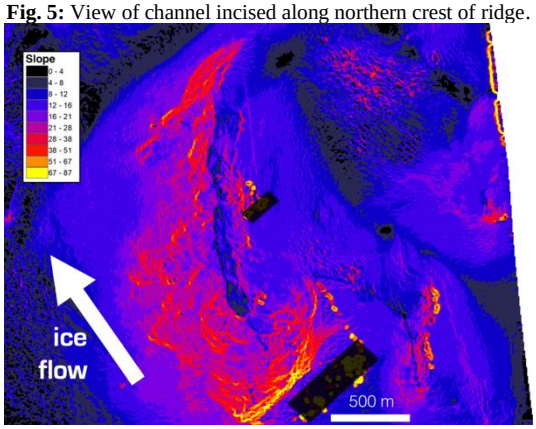

Fig. 6: Slope map derived from HiRISE DEM. DEM artifacts caused by shadow edges have been partially obscured by black boxes.

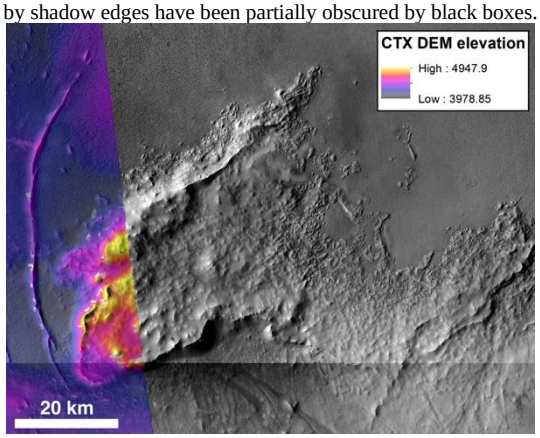

Fig. 7: The V may be a hyaloclastite mound. CTX mosaic and DEM.

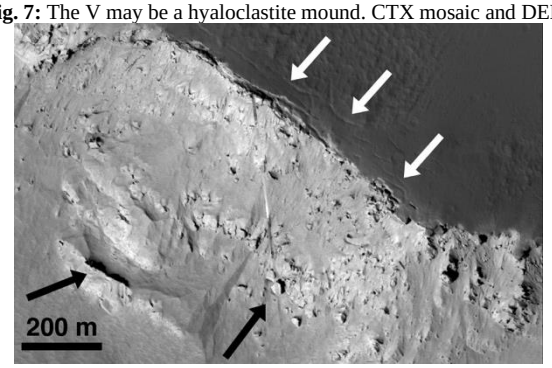

Fig. 8: Fractures in the upper layers of the V (white arrows); slump blocks and boulders (black arrows). HiRISE ESP_066744_1840.

The V: Near the center of the Pavonis Mons FSD is a "V-shaped" plateau **(Fig. 7)** that stands ~200 m above the surrounding terrain, with ridges up to ~100 m higher at the edges. Side slopes are as steep as ~50°.

Two HiRISE images of the edge of the V reveal stacked, cohesive layered material similar to that seen at the W, but with slump blocks and boulders in the talus (**Fig. 8**). Fractures parallel to the scarp at the ridgetop indicate initiation of additional slump blocks.

Discussion: Slopes in the ridge we studied in detail within the W are too steep for the ridge to consist of sublimation till as in the knobby facies [3, 4]. Rather, we interpret it as stacked layers of volcanic material. Due to the lack of an associated lava flow, we interpret the channel (**Fig. 5**) as fluvial. One possible terrestrial analogue for the ridge is Thórólfsfell [22], which formed as a stack of effusive subglacial flows because steep regional slopes allowed meltwater to efficiently drain away from the growing edifice, preventing fragmentation into hyaloclastite. An alternative means for efficient drainage would be required at the Pavonis outcrop, where regional slopes are quite flat. The channel at the north of the outcrop is also more difficult to reconcile with coherent basalt. Our preferred hypothesis is that the outcrop and other ridges in the W are tindar, i.e. hyaloclastite ridges. Their distribution, morphology and morphometry are similar to terrestrial tindar [1], several of which exhibit similar layering [23].

The V may be a hyaloclastite mound or a tuya, with cohesive layers in the uppermost strata. Currently available data show no unambiguous evidence for lava deltas and passage zones, however. This feature could alternatively represent a "sunken-centered flow" as at Arsia Mons [11]. Ongoing work includes detailed mapping of the remaining outcrops in the V landform.

Acknowledgments: We thank the originators and curators of the data [13, 16-19] and tools [15, 20] we used in this work, and the NASA Postdoctoral Program for funding to KES.

References: [**1**] Smellie J.L. & Edwards B.R. (2016) Cambridge Univ. Press. [**2**] Diniega S. & I.B. Smith (2020) *PSS* 182. [**3**] Head J.W. & Marchant D.R. (2003) *Geology* 31(7). [**4**] Shean D.E. et al. (2007) *JGR: Planets* 112(E3). [**5**] Kadish S.J. et al. (2008) *Icarus* 197(1). [**6**] Forget F. et al. (2006) *Science* 311(5759). [**7**] Kadish S.J. et al. (2014) *PSS* 91. [**8**] Werner S.C. (2009) *Icarus* 201(1). [**9**] Pedersen G.B.M. & P. Grosse (2014) *JVGR* 282. [**10**] Fastook J.L. et al. (2008) *Icarus* 198(2). [**11**] Scanlon K.E. et al. (2014) *Icarus* 237. [**12**] Scanlon K.E. et al. (2015) *Icarus* 250. [**13**] McEwen A.S. et al. (2007) *JGR: Planets* 112(E5). [**14**] Scanlon K.E. & Head J.W. (2021), *LPSC LII*, #1259. [**15**] Beyer R.A. et al. (2018) *ESS* 5. [**16**] Smith D.E. et al. (2003), NASA PDS. [**17**] Tanaka K.L. et al. (2014) *PSS* 95, 11–24. [**18**] Edwards C.S. et al. (2011) *JGR*, 116. [**19**] Malin, M. C., et al. (2007) *JGR: Planets* 112(E5). [**20**] Dickson J.L. et al. (2018), LPSC XLIX, #2480. [**21**] Smellie J.L. & Panter K.S. (2021). *Bull. Volcanol., 83*(8). [**22**] Hodgetts A.G. et al. (2021). *JVGR, 411*. [**23**] Schopka H.H. et al. (2006). *JVGR, 152*(3-4).